Effect of Deposition Time On Optical Properties of Chemical Bath Deposited Mercury Sulfide Thin Layers

Haleh Kangarlou (h.kangarlou2020@yahoo.com)
Islamic Azad University

Somayeh Asgary
Islamic Azad University

Research Article

Keywords: Mercury sulfide, optical properties, Kramers-Kronig relations

Posted Date: September 20th, 2021

DOI: https://doi.org/10.21203/rs.3.rs-875077/v1

Abstract

Mercury sulfide films were deposited on amorphous glass substrates from aqueous solutions by chemical bath deposition method (CBD) at same temperature and different deposition times. Produced layers were post annealed at 250°C about one hour. X-ray diffraction (XRD) was used to study of film's crystalline structural. Their optical properties were measured by spectrophotometry in the spectra range of 400-850 nm, Kramers-Kronig method was used for the analysis of reflectivity curves of HgS films to obtain the optical constants of films in order to investigation of relation between deposition time and optical properties. According to X-ray diffraction details, all thin films showed crystalline phase with a preferential growth along the (220) planes. Optical results have been shown photolminisance property for HgS produced thin films. By increasing deposition time, the dielectric property, refractive index and band gap values are increased.

1. Introduction

Mercury sulfide (HgS) is a polymorphic group II–VI semi-conductor. The most stable phases of HgS are α-HgS (trigonal, cinnabar) and β-HgS (cubic, meta-cinnabar), with room temperature energy bandgaps (Eg) of 2.03 eV and 0.54 eV, respectively [1–3]. HgS has wide application in numerous fields as image sensors, as a contact for semiconductor devices, as a binary constituent in ternary compounds for uses in solar cells, in light-emitting devices, as well as in quantification of biomolecules by conjugation on nanoparticles [4-5], electrostatic image materials, ultrasonic transducers, and photoelectric conversion devices [6-7]. Also, HgS is a suitable material in the manufacture of non-linear optical devices to detect infrared signals, as well as piezoelectric transducers, photoelectrochemical cells, etc. [8].

HgS crystallizes in three different structures that among them α-HgS (cinnabar, trigonal type, hexagonal unit cell) and β-HgS (metacinnabar, zincblende type, cubic unit cell) have been most intensively explored.

HgS layers have been prepared by evaporation [9] and sputtering [10] methods by different researches. They are useful in ultrasonic transducers, image sensors [11], electrostatic imaging materials [12], and photoelectric conversion devices.

There are many different methods for determining the optical constants of materials. One of the most common techniques that have been used to determine the optical constants over the whole measurement range is Kramers-Kronig analysis. The present work describes the synthesis of α-HgS thin films by chemical bath deposition method. Kramers- Kronig computational method is used to calculate the optical constants of produced films as a function of deposition time.

2. Experimental Details

Mercury sulfide layers were produced by chemical bath deposition method on glass substrates. Prior to deposition, the glass substrates of (50mm * 25mm * 1mm) were cleaned ultrasonically in hetead acetone

and then alcohol. For synthesis appropriate amounts of mercury chloride solution and Na_2SO_3 are separately prepared. Formed mixture is thoroughly stirring for several minutes in order to dissolve and solution to become homogeneous. Distilled water also added to for preparation of solution. These solutions were mixed in a beaker and stirred well for a few minutes. The deposition bath was continuously stirred and heated up to 75°C temperature and kept constant in this temperature. Cleaned substrates put in to aqueous solutions vertically by holders. We used 50, 100 and 150 minutes different deposition times. Other deposition parameters were: [mercury chloride] = 0.05M; [Na_2SO_3] = 0.01 M; pH = 2-3; Produced layers were at 250ºC for one hour. Crystal and phase structure of the deposited layers were identified using an X-Ray Xpert MPD diffractometer (CuKα radiation, λ=0.15406 nm) with step size of 0.03 and count time of 1s per steps. Reflectance of the layers was measured with UV-VIS spectrophotometer (Hitachi, U-3310) instrument. In order to obtain optical constants of HgS thin films Kramers-Kronig analysis was carried out on the reflectance spectra on the samples.

3. Results And Discussion

3.1. X-Ray Diffraction analysis

For investigation the crystalline structures of the deposited thin films, XRD measurements were used at room temperature. Figure 1 shows the X-ray diffraction pattern of HgS/glass thin films produced at different deposition times of 50, 100 and 150 minutes. The XRD pattern shows single crystal of α phase of HgS with only (220) reflections characteristic at $2\Theta=32.44^{o}$ which are in good agreement with the JCPDS-pattern (JCPDS file No.: 73-1593). The films tend to crystalized in a certain direction.

As shown, increasing deposition time gradually leads to higher lattice volume as specified by peak shift towards lower diffraction angle (higher d value) due to increasing the compressive stress in the films.

3.1.2. Energy dispersive X-ray spectroscopy

EDAX results are shown in figure 2. In agreement with our purpose, the peaks of Hg and S were present in the spectrum with the large peak of Si. The Hg and S peak intensity increased by increasing deposition time. We can consider that by increasing deposition time, oxygen can also come from the air during the deposition process and resulting in lower O amount. The layers deposited at 50 minutes have a more oxygen-rich composition. The increased in deposition time lead to decrease in oxygen content in the layers.

3.3. Optical properties with Kramers-kronig relations

The relation between deposition time and optical properties were investigated. In this work Kramers-Kronig relations were used to calculate the phase angle θ (E) [13-14]:

$$\theta(E) = -\frac{E}{\pi}\int_0^{E_2}\frac{\ln R(E) - \ln R(E_0)}{E^2 - E_0^2}dE + \frac{1}{2\pi}\ln[\frac{R(E)}{R(E_2)}]\ln\frac{E_2 + E}{|E_2 - E|} + \frac{1}{\pi}\sum_{n=0}^{\infty}[4(\frac{E}{E_2})^{2n+1}](2n+1) \qquad (1)$$

Where E denotes the photon energy, E_2 the asymptotic limitation of the free-electron energy, and R(E) the reflectance. Hence, if E_2 is known, the θ (E) can be calculated. Then the real and imaginary parts of the refractive index were calculated, from which other parameters were obtained.

Figure 3 show transmittance and reflectance curves for mercury sulfide layers produced by chemical bath deposition method in different deposition times of 50, 100 and 150 minutes, for this work.

The spectra's are obtained in visible light energy range (1.5-3 eV). As it can be seen from figure 1, before 2 eV, curves have been separated. This region belongs to hot colors as red and infrared. By increasing deposition time, transmittances decreases that are because of configuration of complete layers by increasing deposition time. Also in this range of energy (1.5-2 eV) transmittances are high and are about 80% up to 90%, for the layers produced in this work. Oblique and almost same transmittance and reflectance observe for 2 eV to 2.3 eV energy ranges that belongs to orange color. For 2.3 eV up to 3 eV energies that belongs to violet, blue, green and yellow colors, curves are almost the same and are in straight lines also transmittance of this region is very low and reflectance (figure 3b) is very high, that means mercury sulfide is offended layer in this range, HgS layers are almost transparent in hot color wavelengths and offended in cold color wavelengths. Figure 3 shows the reflectance of mercury sulfide produced

in this work. On the contrary of transmittance curves, there are high reflections for high energies and low reflections for lower energies. In lower energy range by increasing deposition time reflection increases that is because of formation complete layers.

Figure 4 shows the real part of reflective index for mercury sulfide layers produced in this work. Real part of refractive index begins from a minimum and reaches to a maximum and continues in a straight line for all layers. As it can be seen, by increasing deposition time, n has an increasing trend that is because of formation complete and dense layers by increasing deposition time. The results of real part of refractive indices are in agreement with reflection curves.

Figure 5 shows the imaginary part of refractive index (k). These curves are in exact agreement with transmittance curves. In infrared, red and orange energy regions, there is a low extinction coefficient for mercury sulfide layers and the k amounts are almost the same. By increasing deposition time in the range of 2.3 eV- 3 eV energies, transmittance of layers decreases therefor absorbance increases. In the violet, blue, green and yellow energy region, extinction coefficients are high.

Figure 6 shows the real part of dielectric function. All curves begin from a minimum and increase to a maximum. By increasing deposition time real parts of dielectric functions (ε_1) increase, that is because of formation more HgS molecules on layers by increasing deposition time. ε_1 for low energies is almost the same. Figure 7 shows the imaginary parts of dielectric functions (ε_2). For low energies range, ε_2 curves are almost the same. By increasing deposition time, ε_2 curves increases in high energy ranges. ε_2 results are in exact agreement with extinction coefficient curves. Figure 8 and 9 show real parts (σ_1) and imaginary parts (σ_2) of optical

conductivities for layers produced in this work, respectively. By increasing the deposition time, real part of conductivities decrease and imaginary parts of conductivities increase. Results are in the exact agreement with dielectric function curves. There are a high conductivities for violet, blue, green and yellow colors and low conductivity for orange, red and infrared colors. Hg atoms for layer produced at 50 minutes have high densities and S atoms in same layer have low densities. For layer produced at 100 minutes, number of Hg atoms decrease and number of HgS molecules increases and also for layer produced at 150 minutes, number of Hg atoms has low densities and HgS molecules configure more on layer.

Figure 10 shows the absorption coefficient for mercury sulfide layers produced in this work. In high energy ranges, by increasing deposition time absorption coefficient decreases. There are high absorbance for this region, Therefor mercury sulfide layers for violet, blue, green, yellow colors are offended and for orange, red and infrared colors are transparent. As it can be seen from all optical results, orange is a frontier color for HgS layers and mercury sulfide layers have photolminisance property.

Figure 11 shows the values of band gap energy for the layers produced in this work. By increasing deposition time, present of Hg atoms decrease and formation of HgS molecules increase, therefor dielectric property increases and value of band gap also increases. Table 1 shows the values of bang gap energy for mercury sulfide layers produced in this work.

Table I: Band gap energy values of β- HgS nano layers

Deposition time (minutes)	band gap energy (eV)
50	1.96
100	2.06
150	2.08

4. Summary

Mercury sulfide nano layers were deposited from aqueous solution using CBD method, at different deposition times 50, 100 and 150 minutes. Produced Nano layers post annealed at 250°C about one hour.

The optical properties of produced layers were calculated by Kramers-Kronig relations on reflectivity curves in visible light energy range. Mercury sulphide layers had photolminisance property. Produced layers were transparent for hot colours and were offended for cold colours. Orange is frontier colour for produced layers.

References

1. H. Wang, J. JieZhu, A sonochemical method for the selective synthesis of α-HgS and β-HgS nanoparticles. Ultrason. Sonochem. **11**, 293–300 (2004)
2. S.H. Choe, K.S. Yu, J.E. Kim, H.Y. Park, W.T. Kim, Optical properties of HgS and HgS: Co^{2+} crystals. J. Mater. Res. **6**, 2677–2679 (2011)
3. K.J. Siemsen, H.D. Riccius, 1970, Preparation and Optical Properties of Evaporated β-HgS Films, 37, 445–451
4. J.O. McCaldin, J.S. Best, 1977, Mercury chalcogenide contact for semiconductor devices, US4123295A
5. C. Xu, I.K. Sou, K.S. Wong, H. Wang, Z.U. Yang, G.K.L. Wong, 1995, Light emitting material, US5540786A
6. N. Tokyo, Jpn. Kokai Pat. 75130378 (C1.H01L.C01B), 1975
7. N. Tokyo, K. Azkio, Jpn. Kokai Pat. 7855478 (C1.C23C15/00), 1978
8. G.D. Boyd, T.H. Brigdes, E.G. Burkhardt, J. Quantum Electron. **4**, 515 (1968)
9. A. Chemseddine, R. Morinean, J. Livage, Electrochromism of colloidal tungsten oxide. Solid State Ionics **9**, 357–361 (1983)
10. M. Kaelin, D. Rudmann, A.N. Tiwari, Low cost processing of CIGS thin film solar cells. Sol. Energy **77**, 749–756 (2004)
11. S.S. Kale, C.D. Lokhande, Preparation and characterization of HgS films by chemical deposition. Mater. Chem. Phys. **59**, 242–246 (1999)
12. S.S. Kale, H.M. Pathan, C.D. Lokhande, Thickness dependent photoelectrochemical cells performance of CdSe and HgS thin films. J. Mater. Sci. **40**, 2635–2637 (2005)
13. H. Kangarloo, S. Rafizadeh, B. Salimi, Optical properties of titanium oxide nano layers. Proc. 3rd WSEAS Int. Conf. on Eng. Mechanics, Structures, and Eng. Geology (EMESEG'10), World Scientific and Engineering Academy and Society (WSEAS), Stevens Point, Wisconsin, USA (Latest Trends on Engineering Mechanics, Structures, Engineering Geology). (2010) 305–309
14. H. Entezar Mehdi, P. Esmaili, M. Nasiri Sarvi, S. Asgary, Effect of Sputtering Pressure on Structural and Optical Properties of Silver Oxide Thin Films; Kramers-Kronig Method. Journal of Optical and Quantum Electronics **50**, 344–353 (2018)

Figures

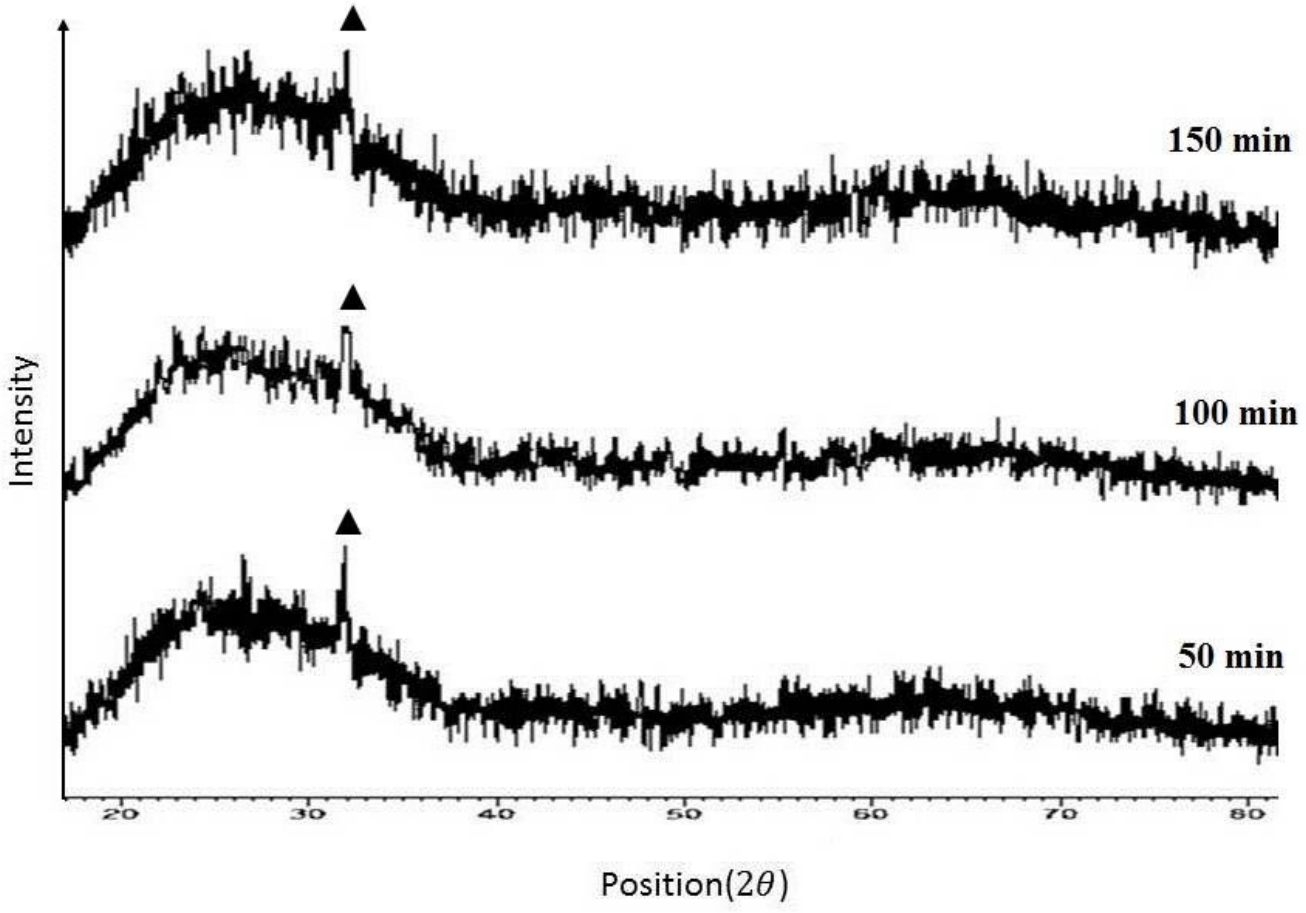

Figure 1

The XRD spectra of mercury sulfide layers produced by CBD method at different deposition times

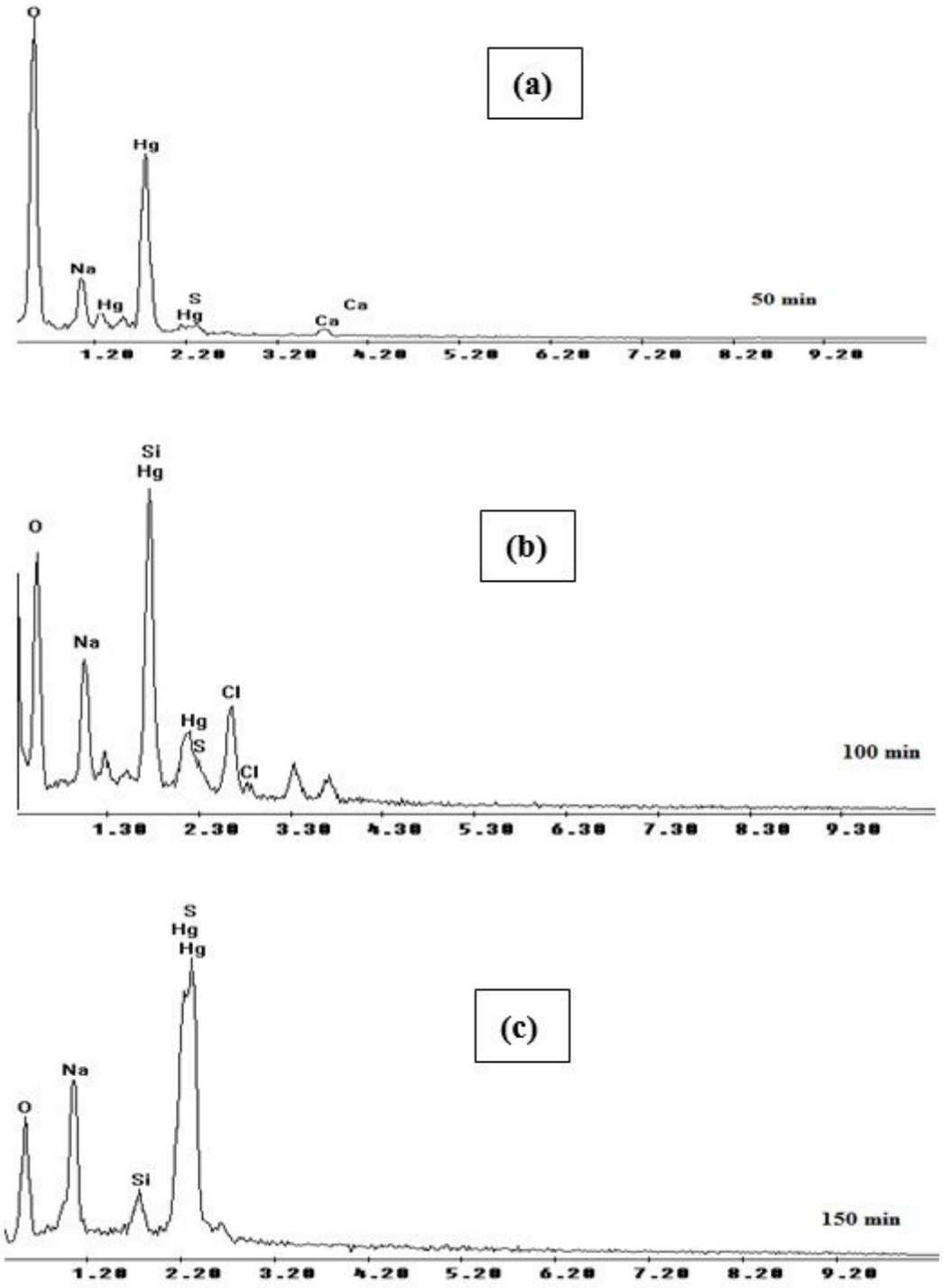

Figure 2

The EDAX images of mercury sulfide layers produced by CBD method at different deposition times

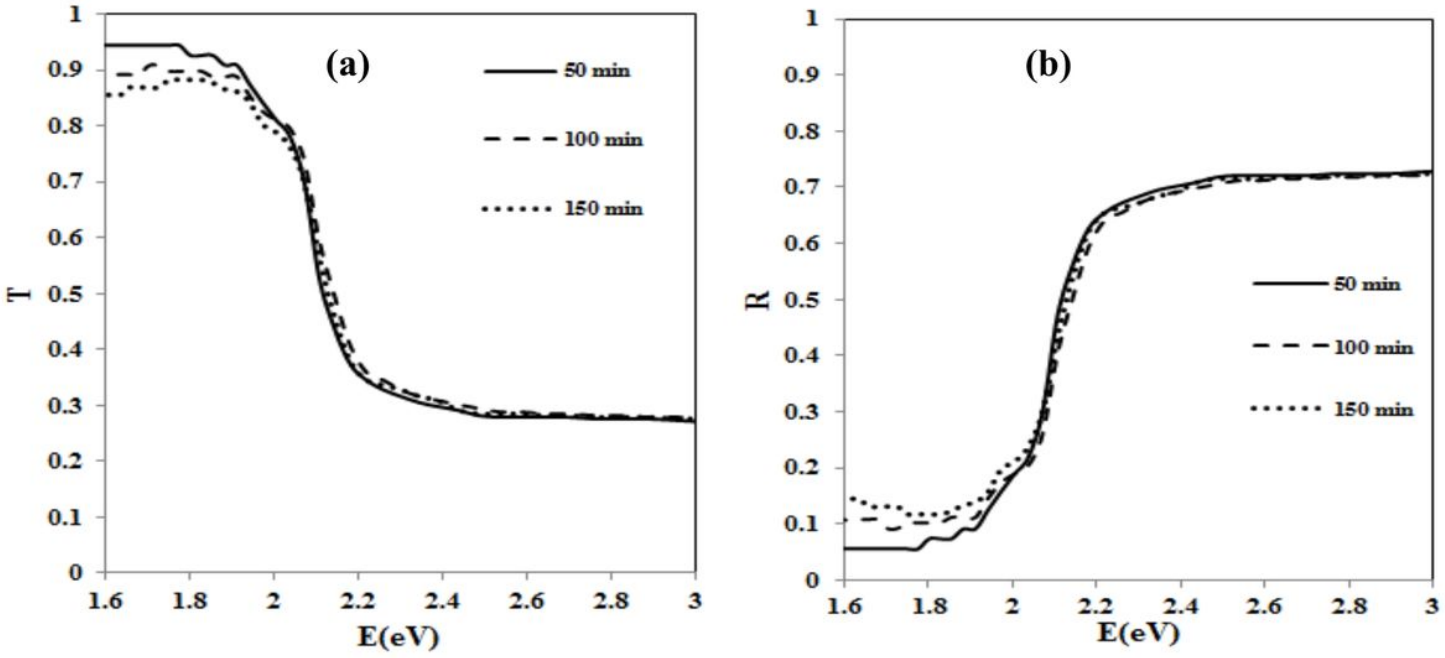

Figure 3

The a) transmittance and b) reflectance of mercury sulfide layers produced by CBD method at different deposition times

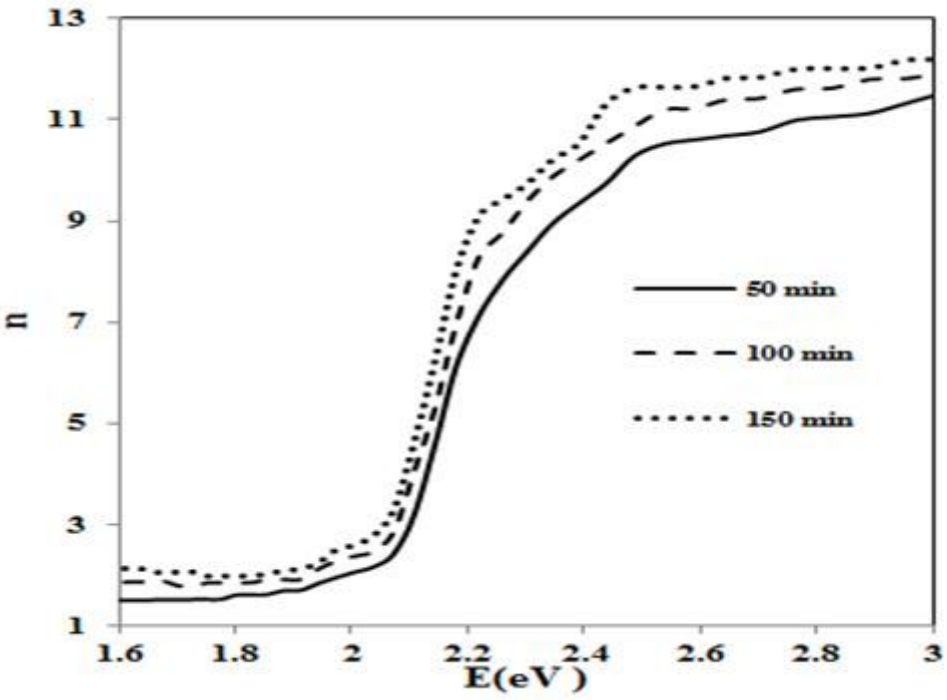

Figure 4

The real part of refractive index of mercury sulfide layers produced by CBD method at different deposition times

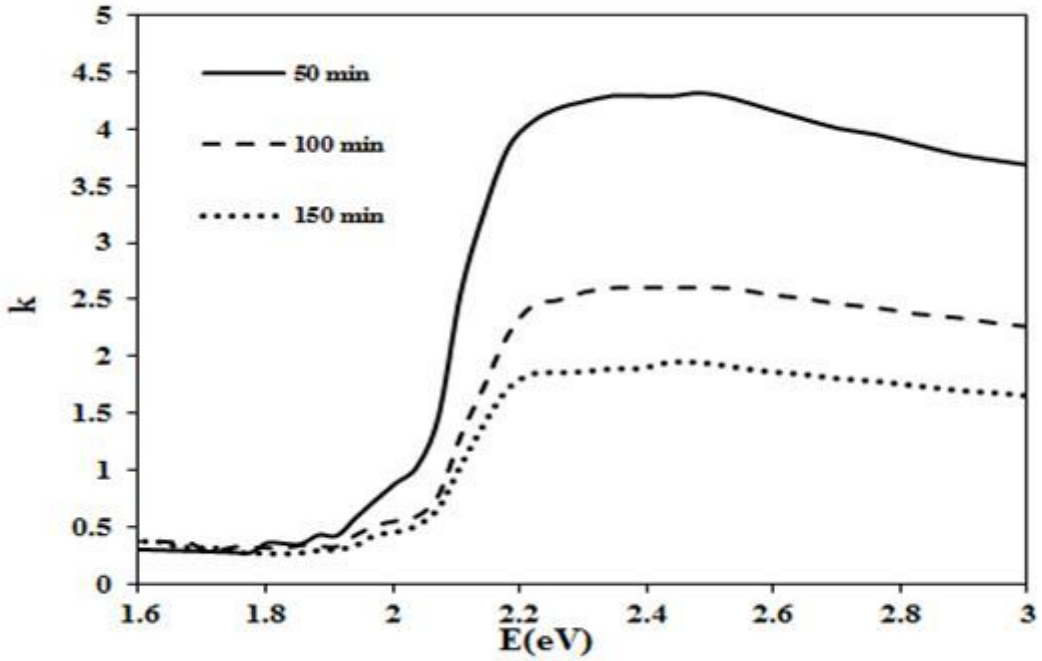

Figure 5

The imaginary part of refractive index of mercury sulfide layers produced by CBD method at different deposition times

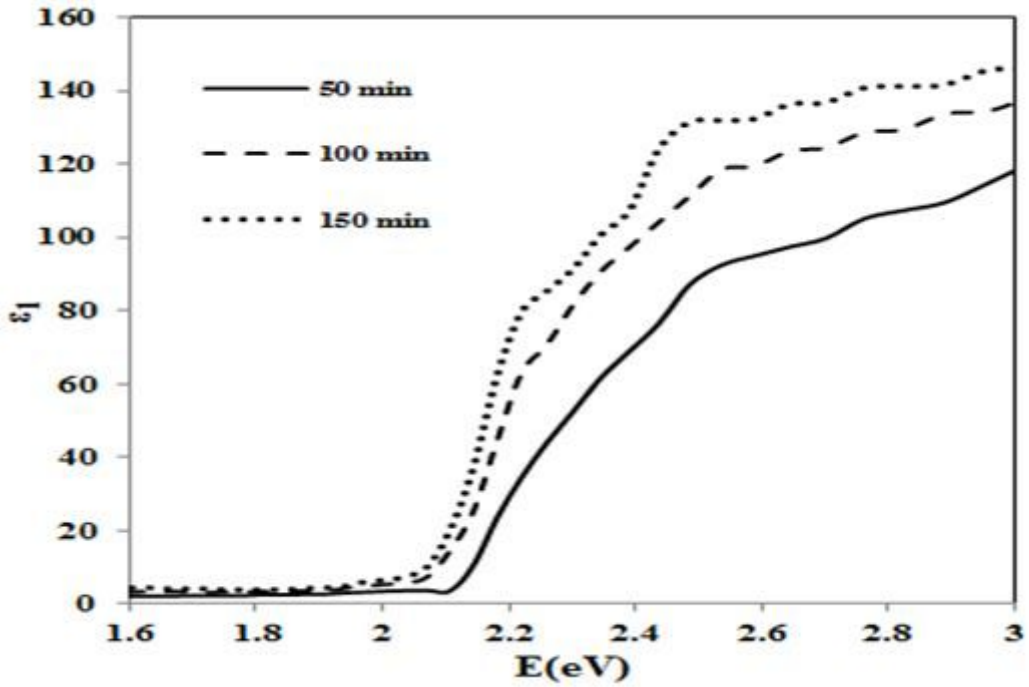

Figure 6

The real part of dielectric constant of mercury sulfide layers produced by CBD method at different deposition times

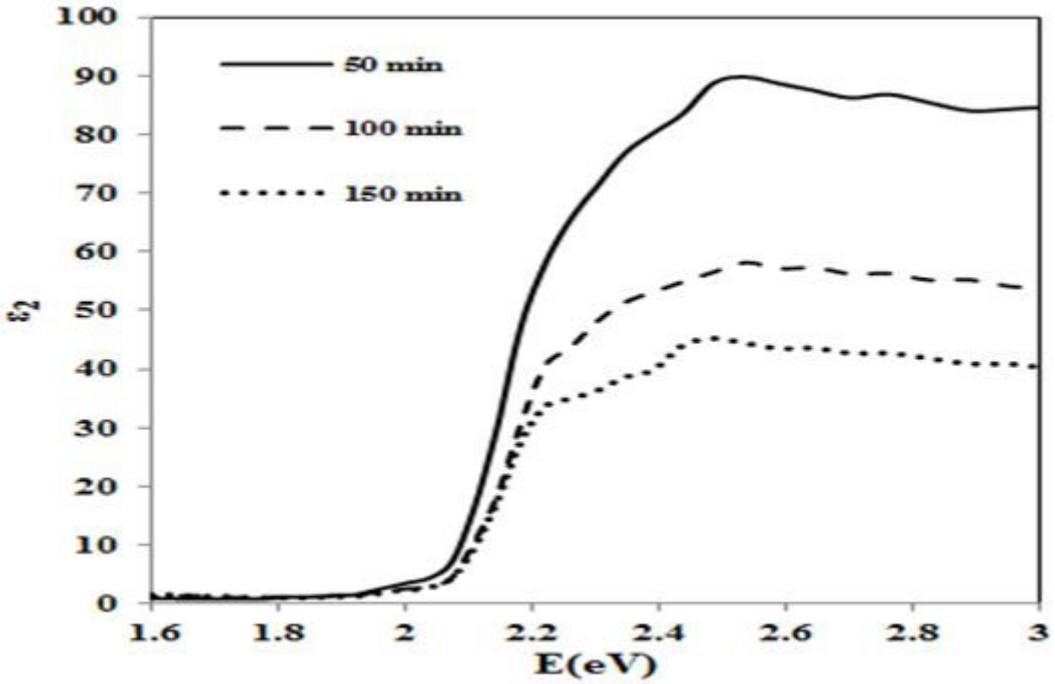

Figure 7

The imaginary part of dielectric constant of mercury sulfide layers produced by CBD method at different deposition times

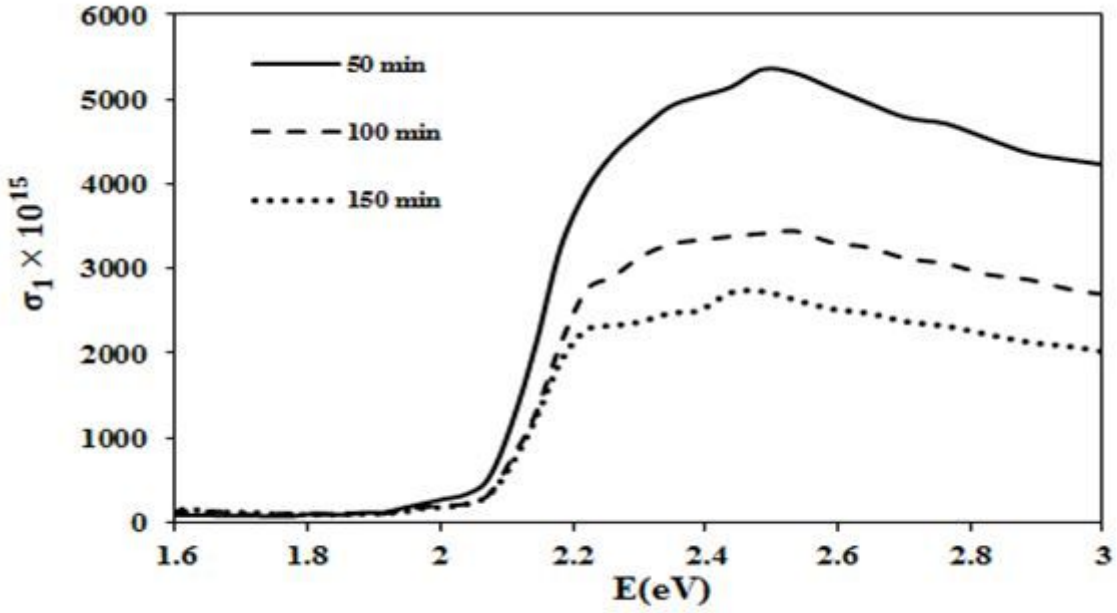

Figure 8

The real part of conductivity index of mercury sulfide layers produced by CBD method at different deposition times

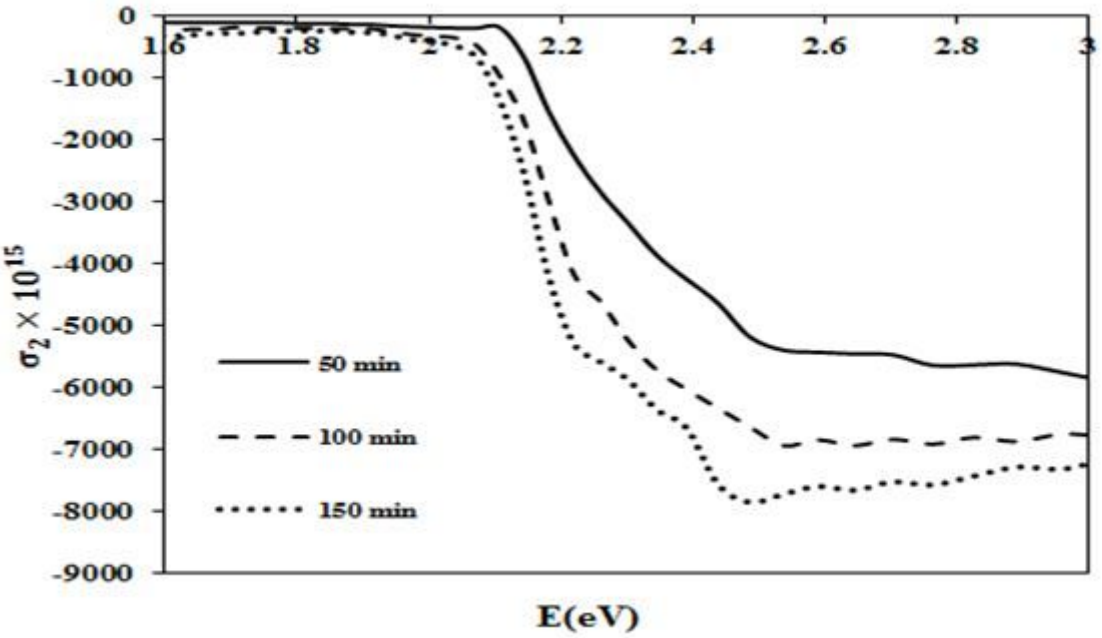

Figure 9

The imaginary part of conductivity index of mercury sulfide layers produced by CBD method at different deposition times

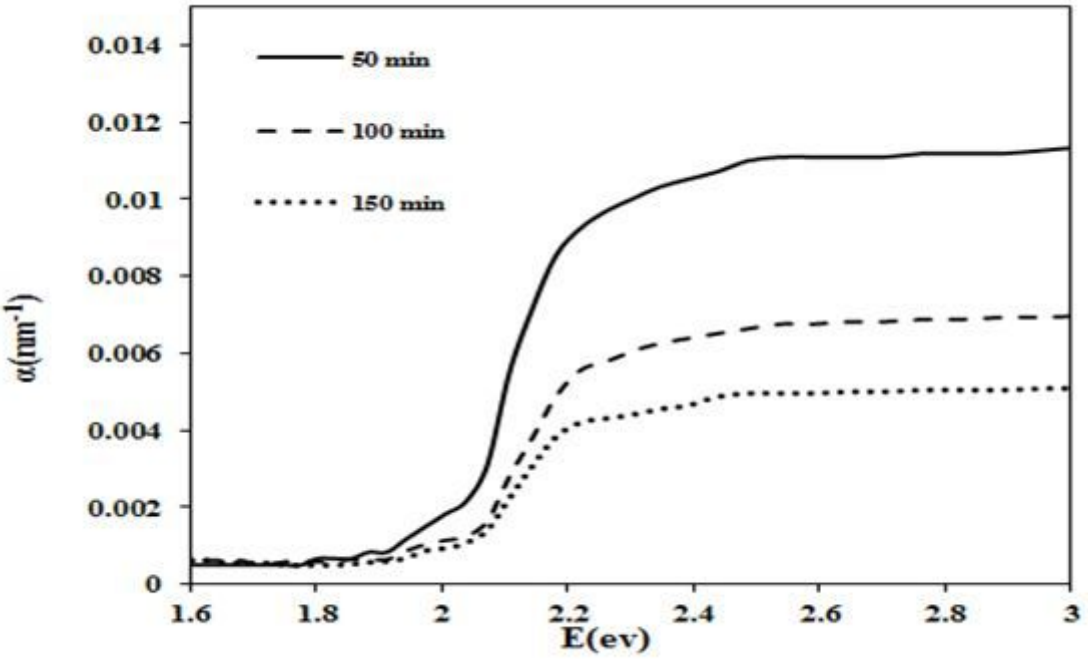

Figure 10

The absorption coefficient of mercury sulfide layers produced by CBD method at different deposition times

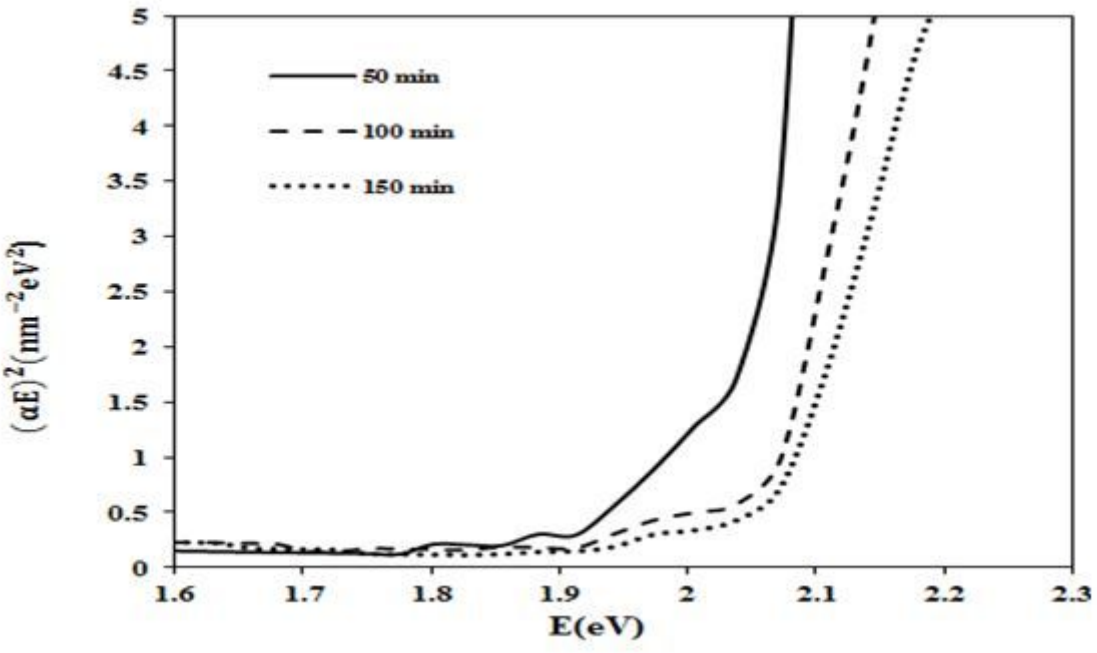

Figure 11

The values of band gap energy of mercury sulfide layers produced by CBD method at different deposition times